

DEVELOPMENT OF FLOWABLE CARBON FIBER MATERIALS

Hamid G. Kia*

Selina Zhao**

General Motors R&D Center Warren MI

Hugh MacDowell***

Detroit Engineered Products, Inc

ABSTRACT

Reducing the fabrication cost is a major step towards reducing the final piece cost for carbon fiber reinforced polymer composite products. In this report we introduce a new family of carbon fiber composites that is flowable and moldable similar to short fiber composites. However, the molded panels have properties at par with hand-layup carbon fiber composites. This goal has been achieved by perforating unidirectional carbon fiber prepregs to a predetermined fiber length distribution. A perforating machine has been designed, built, and utilized to produce the desired product. Furthermore, a lightweight flowable core material has been formulated and produced to be used in a sandwich structure along with the flowable carbon fiber prepreg as the face sheets. Using these materials, 12x12 inch plaques were molded and tested for mechanical and physical properties. Also, structural beams were molded and tested in the three-point flex mode for performance confirmation. The results show that this family of carbon fiber composites can enable net shape molding with fast cycle times of less than 3 min without, for the most part, scrap or offal. Furthermore, the low-pressure molding capability of these materials enable the use of low cost tooling, which, specifically at low volumes, enhances resultant cost savings.

* Retired

**Speaker

***Currently at Continental Structural Plastics Inc.

INTRODUCTION

Carbon fiber composites can deliver extensive mass savings over traditional steel designs by as much as 65%, which makes them the most effective solution for mass reduction. However, the associated cost has proven to be a major hindrance for high volume applications of these materials. The final piece cost has many elements, but it can be broken into two major categories, i.e, material cost and fabrication cost. Surprisingly enough, the fabrication cost at times could claim more than 80% of the piece cost.

Reducing the material cost has been to some extent successful by focusing on reducing the cost of producing carbon fibers [1-5]. That effort however is reaching a plateau with marginal reduction in fiber cost, which indicates other avenues must be explored. On the other hand, the fabrication cost, and more specifically, the role of the material on fabrication complexity has not been sufficiently addressed, which is the subject of the current investigation.

In general, material characteristics dictate the fabrication method and the subsequent associated challenges. Therefore, in order to simplify the fabrication method, one has to focus on materials from the processing point of view. The processing method is determined by the type of resin and fiber. In general, composites with short fiber length and low fiber content, have a fast molding cycle time. However, the performance of the molded parts is not as good as the ones with long fibers and a high fiber content. In contrast the composites with long fibers and a high fiber loading require a long cycle time. A good example of such contrast can be found by comparing a unidirectional carbon fiber prepreg/epoxy system with a random chopped fiber/epoxy sheet molding compound (SMC). The former requires a hand-layup operation with some 30-min cycle time, whereas the latter can be compression molded with much faster cycle time. However, the properties of the hand-layup molded parts are much higher than the compression molded parts [6-10]. It would be very desirable to have a material that can be molded with the SMC processing method and yet can deliver parts with properties similar to panels produced with the hand-layup method. To that end one has to reexamine how carbon fiber attributes to the properties of polymer composite parts.

Single filament carbon fiber in a compatible polymer matrix has a critical fiber length of less than 1 mm [11, 12]. Which means that if a single filament is longer than 10 mm, to overcome the end effects, it will act as if it is continuous [13]. This implies that if a polymer composite sheet can be produced with a staggered fiber distribution shown in Figure 1, it will behave as if the fibers are continuous with

associated superior properties.

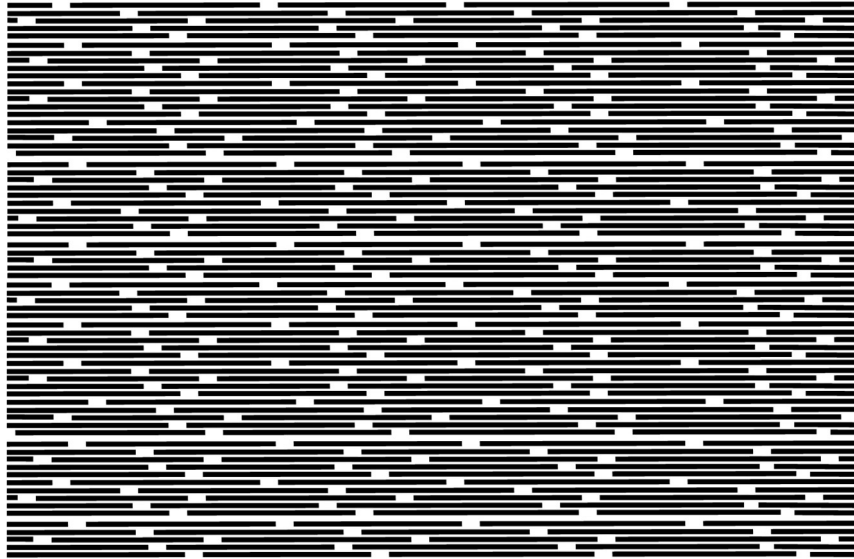


Figure 1. Schematic representation of fiber discontinuity with a staggered pattern

Producing such a composite is, however, a major challenge. To that end, in previously published patent applications [14-15] a few methodologies were proposed. In the first disclosure [14] a few methods were described for imbedding weak points in the length of the precursors such that when they are processed, the resultant carbon fiber could be easily broken with a random pattern into a predetermined length. In the second disclosure [15], the emphasis was on methods of disrupting the oxidation and carbonization processes such that the resultant carbon fiber would have weak points that can render random breakage of the fibers to a predetermined length. Such treatment of precursors and disruption of the oxidation and carbonization inherently narrows down the processing window of carbon fibers. In order to overcome that, in another patent application [16], it was proposed to have a sheath/core structure for the precursors such that the broken core will be protected during the carbonization process. These suggested methods, however, require extensive development and undertaking by the carbon fiber manufacturers, which has not transpired. Therefore, as a short-term measure, a less challenging solution has been proposed [17], which is being addressed in the current study. In this method, unidirectional carbon fiber prepreg sheets are perforated with a predetermined pattern to deliver randomly disrupted carbon fiber.

With the goal of improving the processing of carbon fibers, stretch breaking of fiber tows have been studied [18-19]. Testing of these stretch broken carbon fibers showed that mechanical properties were not compromised. However, the added processing cost was found to be excessive, while the

flowability improvement was not significant enough to justify the added expenses. The reason for insufficient flowability was attributed to the inconsistency in fiber length distribution. As a result, this methodology has not been practiced in the industry.

In contrast, the methodology devised in this project can deliver reproducible fiber length as designed, which enables consistent flowability during the molding operation as well as consistent quality for the molded products. Furthermore, the stretch broken fibers are difficult to process in the downstream operations such as prepreg making process or woven fabric production. Whereas, the material in our process is ready for molding and part fabrication. In this report we will describe the development of these materials and present the description of the equipment which was designed and built for the purpose of producing these flowable carbon fiber prepregs. Also, we will show how a flowable sandwich structure was devised and will present the physical and mechanical test results for the molded plaques and beams.

MATERIALS

Carbon fiber prepreg

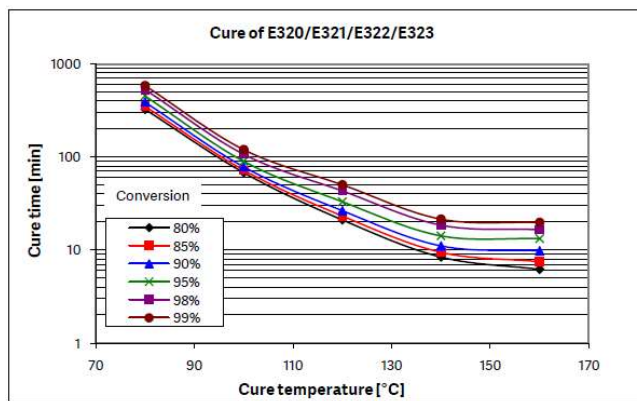
Prepreg is the common terminology for reinforcing carbon fibers which have been pre-impregnated with a resin system that already includes the proper curing agent. It has been used extensively in the aerospace and performance vehicles to meet demanding requirements. Among these materials, unidirectional prepregs are typically long, continuous fiber sheets that are stacked to provide the desired thickness and mechanical properties of the final part. In this work, four unidirectional prepregs from SGL were selected, which are SIGRAPREG®CU200-0/NF-E320/35%, SIGRAPREG®CU200-0/NF-E420/40%, SIGRAPREG® CU200-0/NF-E420/45%, and SIGRAPREG®CU200-0/NF-E501/35%. E320, E420 and E501 are the designation for the three types of resin systems. All of them have an area weight of about 200 g/m². The percentage number in the materials trade name designates the resin content percentage by weight for each system.

E320 resin is a highly toughened epoxy based system with a typical curing temperature of 125°C for 1 hour. The desired properties could be reached by setting the curing condition at various temperatures ranging from 80°C to 160°C. The glass transition temperature (T_g) of E320 is 120°C. E501 resin is also an epoxy based system and is formulated for low temperature cure and applications which don't require high temperature exposure. The glass transition temperature (T_g) of E501 is 110°C.

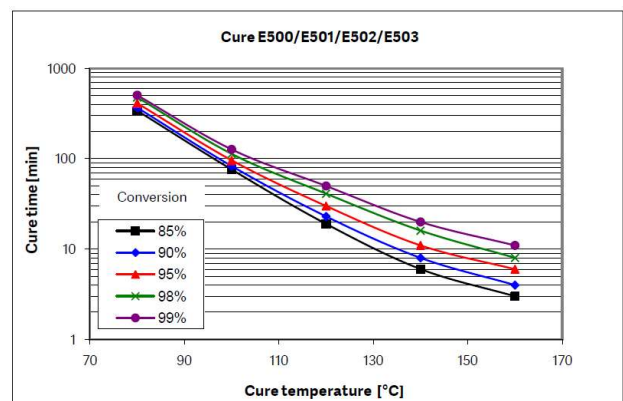
E420 resin is a rapid curing epoxy based system, such that the curing can take place within 3 minutes at 150°C. Even shorter cycle times could be achieved if an appropriate post-cure is applied. The minimum viscosity at 95°C measured by the parallel plate rheometer at 1°C /min is 2 Pa·s. The

glass transition temperature (T_g) measured using DSC at $10^\circ\text{C}/\text{min}$ heating rate is 153°C . It could reach the gelation point at 140°C in 80 second. Figure 2. shows the curing profiles for each resin system, which were used to determine the appropriate molding conditions for each material. As is shown in Figure 2 (c), due to the fast curing rate of E420, a different conversion vs. time scale is adapted. Figure 3 illustrates the complex viscosity of E320, E501 and E420 as the function of temperature, in which E320 and E420 have a lower viscosity compared to E501 at temperatures below 90°C .

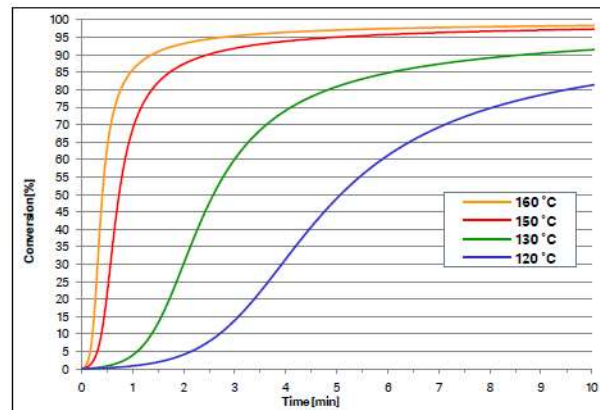
With the goal of finding out the ideal viscosity level in combination with resin curing kinetics, which could maximize the fiber flow during the molding process, studies were conducted using these three resin systems.



(a). Cure kinetics curve of E320



(b). Cure kinetics curve of E501



(c). Cure kinetics curve of fast cure resin system of E420

Figure 2. Cure kinetics curves of a) E320. b) E501, c) E420. (b).

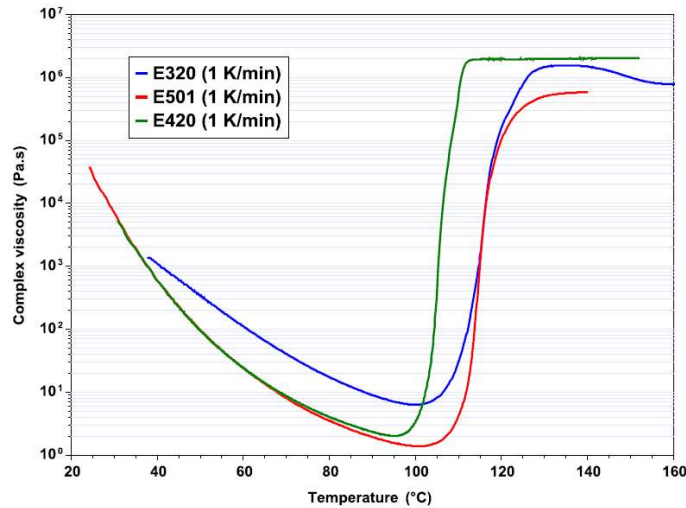


Figure 3. Viscosity curves of E320, E501 and E420

Lightweight flowable core

A lightweight core was formulated and produced in combination with the flowable prepreg skin layer with the goal of creating a flowable sandwich structure. The core material consisted of an epoxy polymer matrix and hollow glass microspheres. As the first step, a standard Bisphenol A diglycidyl ether (DGEBA) resin (DOW 383 epoxy) was mixed with a hardener, Methyltetrahydrophthalic Anhydride (MTHPA), with a part ratio of 100:85. Then, 1 part of air release agent BYK-A 560 was added to enable degassing. S28HS glass microspheres from 3M were then thoroughly mixed with the epoxy resin at 50% by volume (20% by weight). The glass microspheres have 30 micron nominal particle size diameter with an 0.28 g/cc density, and have a 3000 psi crush strength. Their low density and high crush strength are suitable for our application which does not require a high shear mixing load. In order to match the color between the core material and the prepreg, 3% by weight carbon black was added to the paste of epoxy and glass bubbles. The well mixed core material was then placed in a vacuum chamber of 20-25 in-Hg for 15 minutes of degassing.

Based on the viscosity and curing kinetics of the core material, an extra B-staging step was adapted such that the core material would have the same rheological behavior as the carbon fiber prepreg in order to flow the fibers. The outcome of this B-staging process is to increase and build the resin viscosity near its gelation point. Rheological measurements were conducted at several isothermal conditions, which were intentionally lower than the molding temperature in order to widen the processing window, and to have a better control over the polymerization reaction during the B-staging. Based on the rheological studies shown in Figure 4, a 50-min B-staging at 90°C was found to be most suitable to achieve maximum fiber flow. The final core material viscosity after 50 minutes

at 90°C was 100 Pa·s.

The thickness of the B-staged core material was controlled using a 2mm deep plaque mold with lateral dimensions of 25 by 25 cm. After the mixing, the paste was poured into the plaque mold and placed in a heated hand press to compress the resin paste into a 2mm thick sheet at the onset of B-staging. At the end of the B-staging step, the core was removed from the plaque mold and stored in a freezer. The control of the core material thickness is crucial because, otherwise, the exothermic reaction varies from location to location. This will result in a non-uniform polymerization during the B-staging process, which in turn results in having a non-homogenous viscosity in the core sheet.

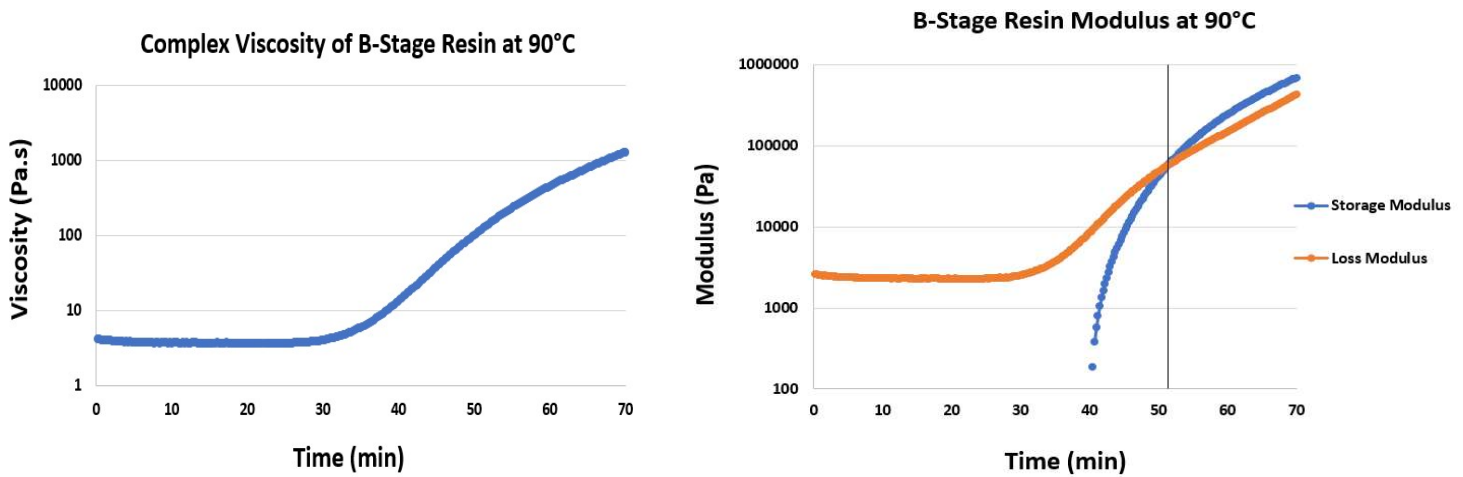


Figure 4. Rheology behavior of the resin under 90°C B-Stage condition

EXPERIMENTAL

Pattern development

In the development of the fiber cutting pattern, there are a few subject matters which have to be considered. The fibers cannot be cut too short because the mechanical properties will be compromised. At the same time, they cannot be cut too long because the flowability will be prohibited. Also, the cut width cannot be too wide because lack of sufficient staggering of the fiber ends will reduce mechanical properties. On the other hand, the cut width cannot be selected to be very narrow as it limits the longevity of the cutting blades. With all these variables in mind, as disclosed in a patent application [17], various cutting patterns were tried and it was concluded that a fiber length of 100 ± 20 mm can enable flowability with minimum loss of properties. Also, it was observed that a small amount of short fibers can further improve flowability. Figure A1 in the Appendix shows the final pattern that was selected. It can be seen that with this pattern, 89.5 wt%

of the fibers have a length of 85 mm, while the remaining 10.5 wt% of the fibers have a length of 10 mm. Figure A2 in the Appendix shows how this pattern was implemented on a cutting head. Locating pins were used to enable precise shifting of the cutting blades.

Equipment design

Using the generated cutting pattern and in collaboration with a supplier (Finn and Fram, Inc.) a perforating machine was designed and built as shown in figures A3-A7 in the Appendix. Although the equipment was manufactured to function in a lab environment, the underlying design of it was such that it could be easily scaled up for high volume production environment. The blades were designed such that the teeth pattern could be easily duplicated. By using locating pins, the blades were positioned with a high precision in the cutting head. Also, because of the presence of the locating pins, only one blade pattern was sufficient to serve the purpose. As a result, the production of the blades with the desired pattern was accomplished with minimum machine time, which is considerable in reducing the cost. This is important for scale up and high volume usage of the cutting head. Also, the cutting head assembly was designed such that the blades could be easily replaced in case of damage. It should be noted that the blades are expected to last very long due to the way they are being used. In this machine the fibers in the prepreg are stretched over an anvil roller. The blades come to contact with the fibers at the apex of the anvil requiring minimum of force to break the fibers. This method of operation increases the longevity of the blades. More details are described in a recent patent application [20].

The machine includes a cutting head with 76 toothed blades. The blades' teeth are 1 mm wide and 9.5 mm apart. Each blade is mounted into the slot between two locator pins on the cutting head and secured using a spacer and a spring in the slot as depicted in Figure 5. The blades are offset and staggered as indicated in the figures shown in the Appendix, using two locator pins. The distance between the two locator pins from center to center is 649mm. As shown in Figure A3, one set of 19 blade offsets is covering 90° of the cutting head cylinder, and as a result it has 4 sets (totaling 76 blades) to cover the whole circumference of the cylinder. A supporting cylindrical anvil roll, which has an elastomeric surface, is connected to a speed control step motor (Figure A6b). The anvil roll is configured to rotate and move the carbon fiber prepreg material from the prepreg roll. Then, the fibers break as they are pressed in a sharp bend under the blades over the elastomeric surface of the anvil roll, as the fibers move between the anvil and the cutting wheel. Because the fibers are broken, not sliced, even dull blades can break the fibers. The perforated material is then collected on the winder roll. Two air cylinders connected to the compressed air provide adjustable pneumatic pressure to the cutting head against the anvil roll whereby the blades perforate the carbon fiber

prepreg. The system accepts rolls of prepreg up to 16" in outside diameter to feed the prepreg into the cutter and a winder that can wind the prepreg on 6" or 10" ID cores. The cores for both the input and winder can be up to 27" long. The perforator unit is mounted on casters, and therefore, is easily portable.

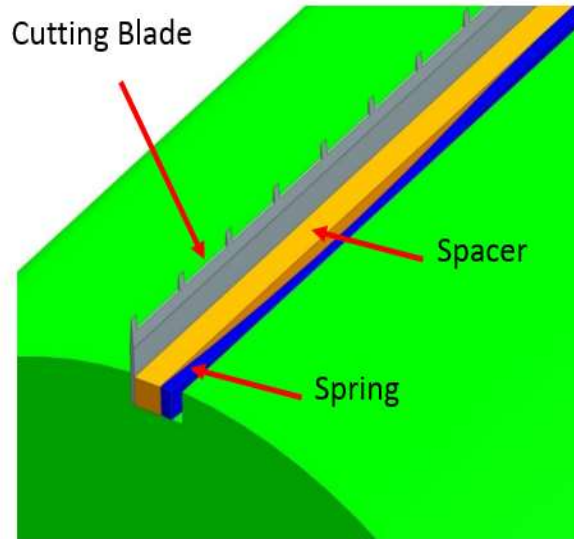


Figure 5. Schematic drawing of cutting blade, spring and spacer. (More details are presented in the Appendix)

RESULTS AND DISCUSSION

Materials screening for flowability

HexMC

Various carbon fiber prepregs from HEXEL and SGL were studied for flowability and cure time. HexMC – i/C/2000/M81 from Hexcel, which is produced to be a flowable material, is a chopped carbon fiber reinforced epoxy system. It has 57% fiber volume content with 2000 g/m² area weight and 1.55 g/cm³ density. Prior to the molding, the process requires an additional step of B-staging. HexMC has to be conditioned (B-staged) at 180 °C for 10 min in the oven to minimize the resin fiber separation and optimize the flow. After this heat treatment, the prepreg is cooled to room temperature, and then loaded into the mold. the molding step requires 20 min of cure at 180 °C followed by a 2-hour post cure at 180 °C, which leads to a very long cycle time. It also requires 1200psi molding pressure, which is relatively high. In the molding trials, the material was cut to have four different initial mold surface coverages, i.e., 50%, 75%, 80% and 100% to evaluate whether it could flow to achieve a fully filled part. Using the 50% and 75% initial mold coverage, the material

could not flow to completely fill the mold cavity. The experiments showed that the minimum initial mold coverage has to be more than 80% in order to achieve a complete part. Therefore, we decided not to use HexMC as a flowable material, and no further evaluation was conducted.

SGL Prepregs

SGL E420 prepreg with 45% resin content by weight was selected to conduct the flowability evaluation due to its fast curing capability. In order to prove the concept of making prepreg flowable by introducing the staggered cut pattern into the continuous fiber filaments, the perforated E420 prepregs were trimmed into 10" by 10" sheets. The charge was stacked up into a 16-layer [0/90/90/0] layup and placed into a 12" by 12" plaque mold as illustrated in Figure 6. It was demonstrated that with the 70% initial mold coverage, under compression, the material can flow to the edges of the mold cavity parallel to the fiber orientation and achieve a fully filled plaque. After the plaque was molded, total of 12 locations were selected and cut for acid digestion analysis in order to generate the local fiber volume fraction map. Using this method, we were able to evaluate the extent of the fiber flow from the center to the edges.

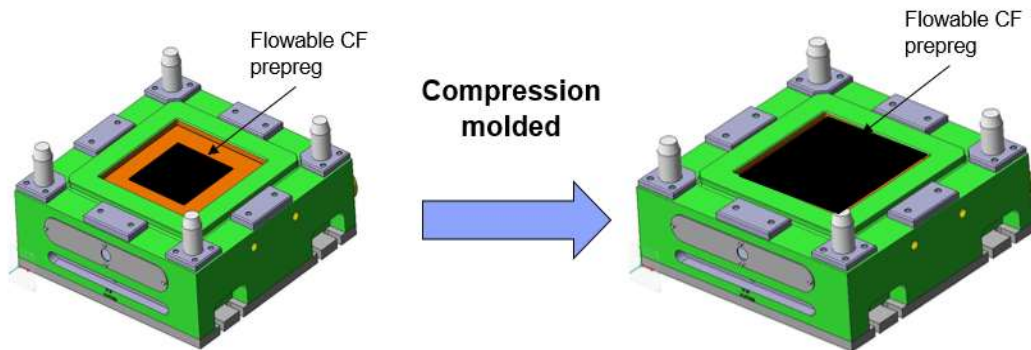
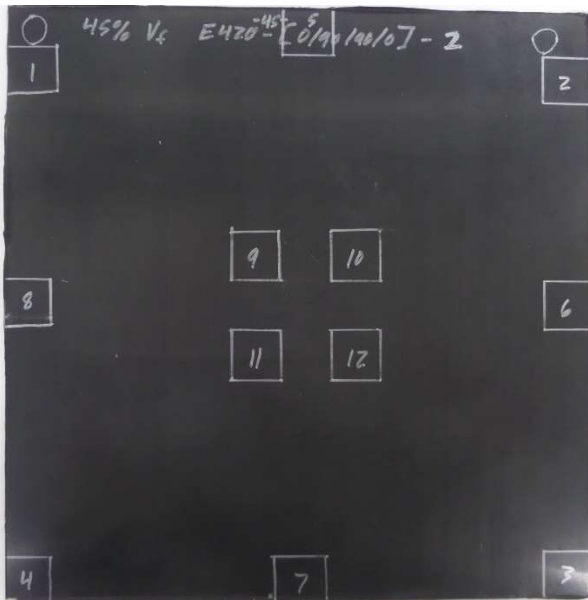
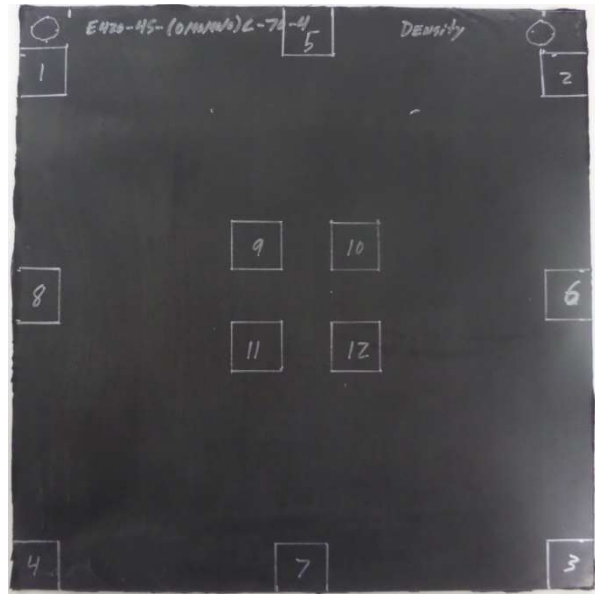


Figure 6. Flowable material in a compression mold

Using E420/45% uncut prepreg with 100% mold coverage, a 12" by 12" plaque was molded (Figure 7a) to establish a baseline for the original fiber volume fraction without any flow. In comparison, the perforated material was molded at 70% mold coverage as shown in Figure 7b. Figures 7a and 7b also depict the 12 locations selected on the plaques for evaluating fiber volume fraction.



(a)



(b)

Figure 7. 12" by 12" molded plaques with [0/90/90/0] layup, a) with 100% initial mold coverage using uncut preregs, b) with 70% initial mold coverage using cut preregs.

Fiber Volume Fraction: Uncut- E420-45-[0/90/90/0]-100%					
y/x	1	2.5	3	4	5
1	48.78		46.71		47.94
2.5		41.90		41.29	
3	42.66				43.71
4		42.11		40.58	
5	53.00		43.26		55.18

(a)

Fiber Volume Fraction: Cut-E420-45-[0/90/90/0] -70%					
y/x	1	5	6	7	12
1	47.20		44.78		45.57
5		41.92		43.50	
6	46.03				44.32
7		43.76		43.91	
12	40.33		42.84		41.68

(b)

Figure 8. Fiber volume fractions at different locations, a) with 100% initial mold coverage using uncut preregs, b) with 70% initial mold coverage using cut preregs.

Figure 8(a) shows that the fiber volume fractions measured at locations #9, #10, #11 and #12 from

the plaque made with no flow and uncut prepreg to be $41\pm 1\%$. And the fiber volume fractions measured at locations near the edges, i.e., #5, #6, #7 and #8, to have an averaged value of 44%. Also, the four corners of the plaque have the highest fiber volume fraction. In Figure 8(b), the plaque that was molded with material flow shows very similar fiber volume distribution compared to the 100% no-flow plaque. Therefore, it demonstrates that the fiber was carried by the E420 resin to the edges of the plaque while maintaining a reasonably uniform fiber volume distribution.

Material characterization

Mechanical properties

Using the selected E420 perforated carbon fiber prepreg with the [0/90/90/0] lay-up of 16 layers and dimensions of 10 by 10 inches, 12X12 inch plaques were molded with initial 70% of mold coverage. All test plaques were molded at 400 PSI and cured at 150°C. The plaques were then cut for tests at the coupon level in order to evaluate the flowable material mechanical properties. In Figure 9, the ATSM standard tensile test results show that the flowable material has a 25% reduction in the tensile strength at break compared to the as received prepreg. However, the tensile modulus remains almost at the same level as the as received prepreg with less than 5% of reduction. This observation is important because the design of many vehicle panels is modulus driven.

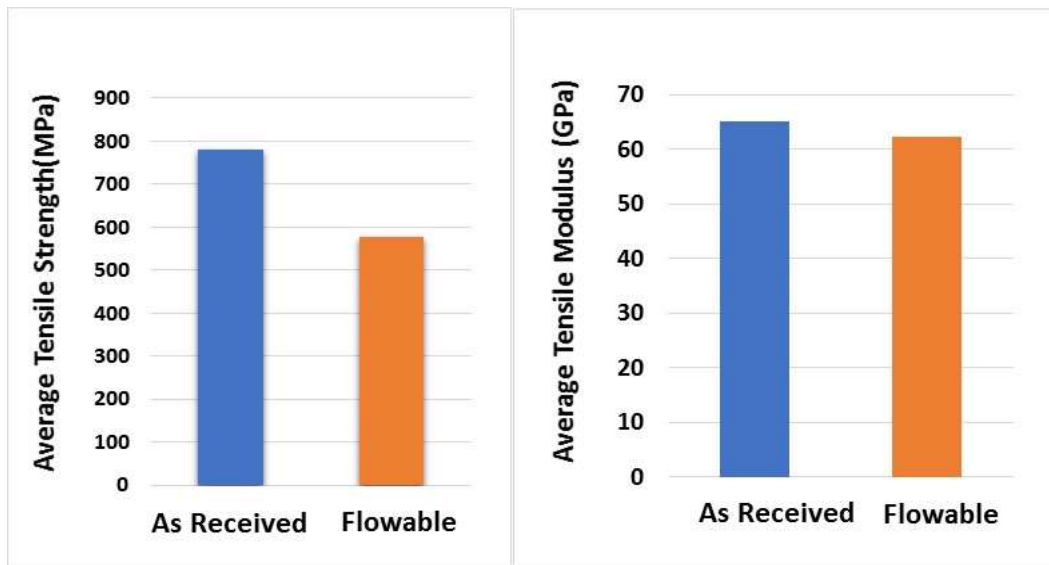


Figure 9. [0/90/90/0] layup coupon level of tensile test results comparison for as received prepreg and the flowable material.

We have evaluated the flowable material properties not only at the coupon level, but also at the

plaque level using the flexural three-point bend test. The flexural tests were conducted using an Instron 5984 test frame with a 150 kN load cell as shown in Figure 10. The diameter of the two supports was 1 inch at a height of 6.75 inches, with a 2.5 inches diameter deflector used to apply the force during the test. The supports and deflector had a width of 10 inches. The support span used during the test was 244 mm with a deflector rate of 12 mm/min. The flexural test was terminated once the load dropped to half of the peak load. We also tested a metal plaque made of Al 6000 series with similar thickness as the baseline study.



Figure 10. The set up for the flexural three-point bend testing of the plaques

Table 1 lists the three-point bend test results. Between the two fiber ply layups of the flowable material, the 0/90 plaque had a much higher maximum load (2.2 kN) than the [+/- 45] sample (1.5 kN). The stretching of the fibers in the [+/- 45] led to a greater strain to failure (1.55%) compared to the 0/90 fibers (1.33%), because of the [+/- 45] layup tends to have a higher elongation than the [0/90] layup.

Both layups show a higher load bearing capability compared to the Al 6000 series while having a lower mass. In Figure 11, it can be seen that the failure has occurred on the back side of the plaque, which was under tension. The crack propagated across the whole width of the plaque linearly and fractured the fiber filaments as if they were continuous instead of breaking the fibers at the perforated points. This observation illustrates that the fiber filaments can carry the load similar to continuous fibers.

Flowable 0/90 and +/- 45 Plaque vs. Al 6000 series			
Sample	Thickness (mm)	Mass (g)	Max Load (kN)
Al 6000 series	2.16	461	1.14
±45	2.43	282	1.5
0/90	2.34	273	2.2

Table 1. Plaque level three-point bend tests on flowable [0/90], [+/-45] material and Al 6000 series

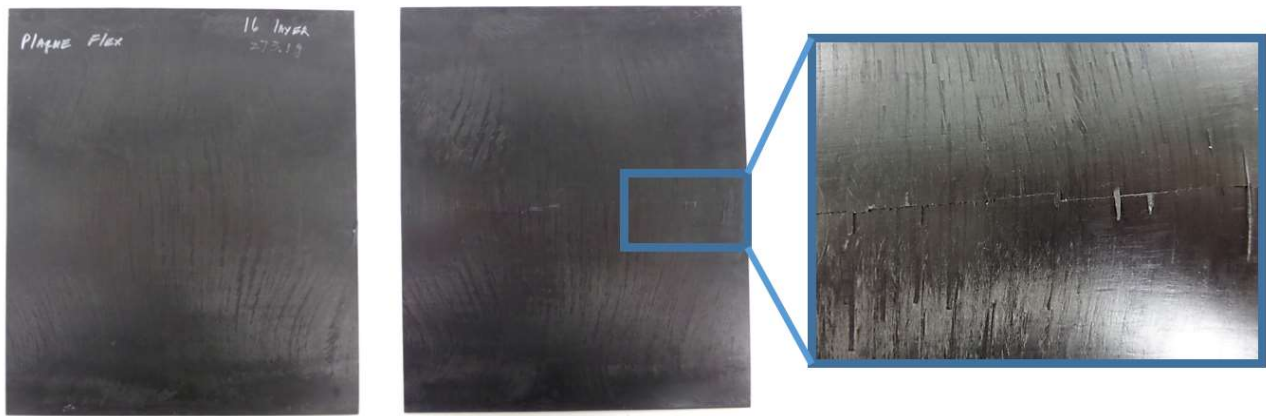
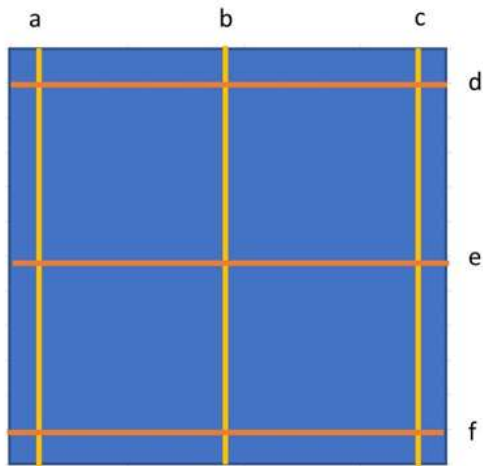


Figure 11. Molded plaque with [0/90] layout after the three-point bend test

Molding shrinkage and CLTE

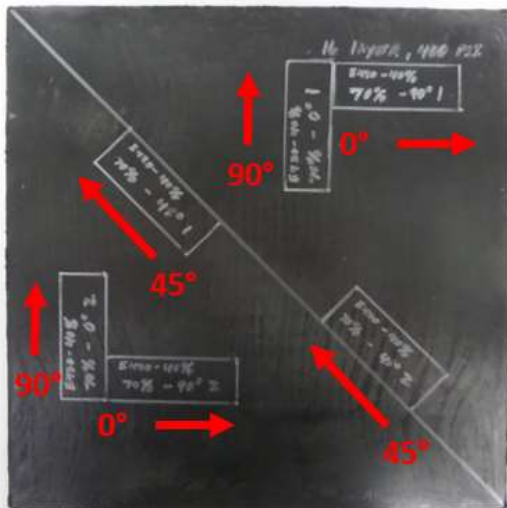
The molding shrinkage and CLTE (coefficient of linear thermal expansion) are two factors that describe the material behavior during molding and in service. The molding shrinkage can be measured using the actual tool dimensions (L_0), subtracted by the part dimensions (L), both at room temperature. We have selected 6 locations as depicted in figure 12 to measure the dimensions on the molded part and the tool. The average molding shrinkage is then calculated based on $(L_0 - L) / L_0$. As can be seen in Figure 12, with the molding shrinkage as low as 0.23%, it can be concluded that the flowable material can deliver dimensionally stable parts.



400psi			
Location	Measured Part Dimension (mm)	Measured Tool Dimension (mm)	Linear Shrinkage
a	305.11	305.73	0.002028
b	305.05	305.83	0.00255
c	305.01	305.82	0.002649
d	305.08	305.79	0.002322
e	305.08	305.72	0.002093
f	305.06	305.75	0.002257
Averaged Linear Shrinkage			0.23%

Figure 12. The molding shrinkage of the flowable carbon fiber material.

The CLTE measurement was conducted by cutting the sample into a 1" by 3" strip along three selected 0°, 45° and 90° orientations. Then, while heating the sample from -40°C to 110°C with 0.23°C/min heating rate, the sample linear expansion was measured. The CLTE was calculated using the slope of the fitted linear line of the measured sample length expansion points. Figure 13 depicts the locations of the samples and the measurement results of these samples. As a reference point, aluminum has a CLTE around $24 \times (10^{-6}/^{\circ}\text{C})$ whereas the SMC has a CLTE around $15 \times (10^{-6}/^{\circ}\text{C})$. The flowable material shows 4-10 times lower CLTE compared to aluminum, and even 3-8 times less than the SMC which is another flowable material. This observation demonstrates good thermal stability for the panels molded with the perforated prepregs.



Sample Name	CLTE (-40°C to 110°C) $10^{-6}/^{\circ}\text{C}$
0° - 1	2.0
0° - 2	3.2
90° - 1	3.3
90° - 2	3.7
45° - 1	5.3
45° - 2	3.4

Figure 13. The CLTE measurement of the flowable material.

SANDWICH STRUCTURE

Using an epoxy polymer matrix in combination with hollow glass microspheres, a lightweight flowable core was formulated as described earlier. The core material was prepared such that it would have the same rheological behavior as the flowable carbon fiber prepreg with the cut fibers. The core material was used in combination with the perforated carbon fiber prepreg to produce a sandwich structure as illustrated in figure 14. It should be noted that conventional composite sandwich structures are not capable of flow in the mold, and this is the first time such a material is being introduced. To demonstrate the value of these materials, a few combinations with different thicknesses for the skin and flowable core were designed to deliver various mechanical and physical properties for different load carrying requirements.

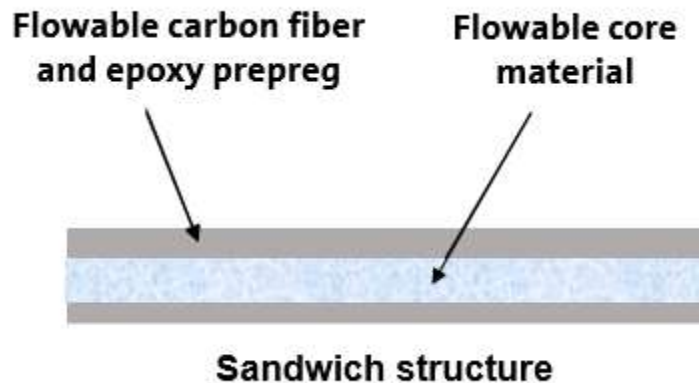


Figure 14. The schematic drawing of the newly developed sandwich structure.

Three-point bend testing of the sandwich structure

The sandwich structures were constructed using 5 types of skin and core thickness ratios as discussed in tables 2 and 3. In all molding conditions shown in Table 3, both skin and core started with the same size, which was 10 by 10 inches to render 70% initial mold coverage. Both skin and core were able to flow and generate a 100% fully filled part using 400 PSI pressure.

The first group of the sandwich structure skins was constructed from a 4-layer prepreg alternating [0/90/90/0] at the top and bottom skin. With this skin configuration, which gives a total of 1.2 mm skin thickness, three types of core thicknesses were adapted which are 1.2 mm, 2.4 mm and 3.6 mm. The second group of sandwich structure skins was made with half of the amount of carbon fiber prepreg, which led to a 2-layer prepreg, [0/90] and [90/0] respectively. With this skin

configuration which produces a total of 0.6 mm skin thickness, two types of core thicknesses were used which were 1.2 mm and 2.4 mm.

Using the above configurations, 12" by 12" plaques were molded, the flexural tests were conducted with 244 mm span width and 12 mm/min rate for evaluation. Based on the cost assumption of each material per kilogram shown in the Table 2, we have calculated the load benefit per dollar of each sample. The summarized results are presented in Table 3.

In configuration #1, the mass reduction was achieved by replacing half of the skin layers with a core, which reduced the mass of the plaques from 273 g to 202 g while still maintaining the same sample thickness thus having very similar flexural load carrying capability, which are 2.2 kN and 1.91 kN. By increasing the core thickness from 1 layer to 2 layers, the flexural load carrying capability was increased to 3.45 kN while the mass (256 g) was still lower than the mass of the solid carbon fiber plaques (273 g). Furthermore, increasing the core thickness to 3 layers of core, resulted in a much higher flexural load carrying capability, 4.26 kN, while it only increased the mass to 308g.

Normalizing the Max Load over the mass, or cost, reveals that the 3-layer core configuration has the highest Max Load/Mass and Max Load/Cost. It implies that this configuration has the best mass and cost benefits under flexural load scenarios. This observation is very important and demonstrates that we could tailor the skin vs. core thickness ratios to meet the specific load requirements of a given application.

Same analysis strategy was applied to the configuration #2 in Table 3. In this configuration, we have further reduced the skin layers thickness to half of the thickness of the skin layers in configuration #1. It can be seen that, the 1-layer configuration has a thickness of 1.9 mm similar to the Al 6000 series plaque, and can carry almost similar load while having one-third of the mass. In addition, the Load/Cost benefit is 1.5 times higher than the Al. In light of these results, it can be concluded that the flowable sandwich structure has good potential to be used for vehicle body panel applications, such as floor pan, battery closure, door panels, etc.

Material	Cost (\$/kg)
Epoxy	5
Glass bubbles	10
Core	5.90
Face sheet prepreg	20

Table 2. The cost assumption for each material. The core was calculated using the assumed numbers for the epoxy and the glass bubbles.

Plaque Flex Test Results						
Sample name	Thickness (mm)	Mass (g)	Maximum Load (kN)	Cost (\$/plaque)	Max Load/mass (N/g)	Max Load/cost (N/\$)
Al 6000 Series	2.16	461.00	1.14	2.30	2.48	496.09
Flowable, no core	2.34	273.10	2.20	5.46	8.07	403.66
Configuration #1- Flowable skin [0/90/90/0]						
1-layer core	2.43	202.10	1.91	3.03	9.44	629.70
2-layer core	3.55	256.10	3.45	3.20	13.47	1077.81
3-layer core	4.71	308.30	4.26	3.44	13.83	1239.53
Configuration #2- Flowable skin [0/90]						
1-layer core	1.93	145	1.04	1.66	7.17	626.51
2-layer core	3.20	223.00	2.18	1.84	9.78	1184.78

Table 3. Summarized flexural performance of each material configuration

Subcomponent level evaluation

In order to evaluate the material flowability in a 3-D geometry, a beam half tool shown in Figure 15a was adapted to conduct several molding trials using four types of materials. The first set of beams, as a baseline, was molded using CF-SMC provided by CSP (Continental Structural Plastics), which was a vinyl ester resin system with 50% by weight carbon fiber. The second set of beams was molded using the solid flowable material with no core, and stacked up into a [0/90/90/0] layup with a 70% initial mold coverage. The third set of beams was molded using the 1-layer core of the configuration #1 sandwich structure material with the same 70% initial mold coverage. The fourth set of beams was molded using the overlapped charge pattern depicted in figure 15b to demonstrate that net shape molding with no offal is another advantage of this methodology.

After the beam halves were molded, they were sanded on the edges and flat sections, wiped with acetone to remove debris, and bonded with Pliogrip 7770 polyurethane adhesive. The beams were then post-cured at 120 °C for 1 hour to fully cure the adhesive.

Three-point flexural testing was conducted on the bonded beams with a 150 kN load cell in an Instron 5984 frame. The test fixture consisted of supports, which were 6.75 inches tall with a diameter of 1 inch and a deflector with 2.5 inches diameter, both the supports and the deflector were 10 inches in length as shown in Figure 16a. The span width of the supports was 360 mm and the rate of deflection during testing was set to be 25 mm/min for all beams.

As shown in figure 16b, the beam molded using the flowable material with no core has the highest specific load which is twice as much as the carbon fiber SMC beam. This observation demonstrates that the flowable carbon fiber maintains its structural load bearing capability at the subcomponent level as well as the plaque level. The beam molded using the sandwich structure and the one with the overlapped charge both showed similar high-performance characteristics. The molding process with the overlap charge configuration verifies that net shape molding with no offal can be delivered with this technology.

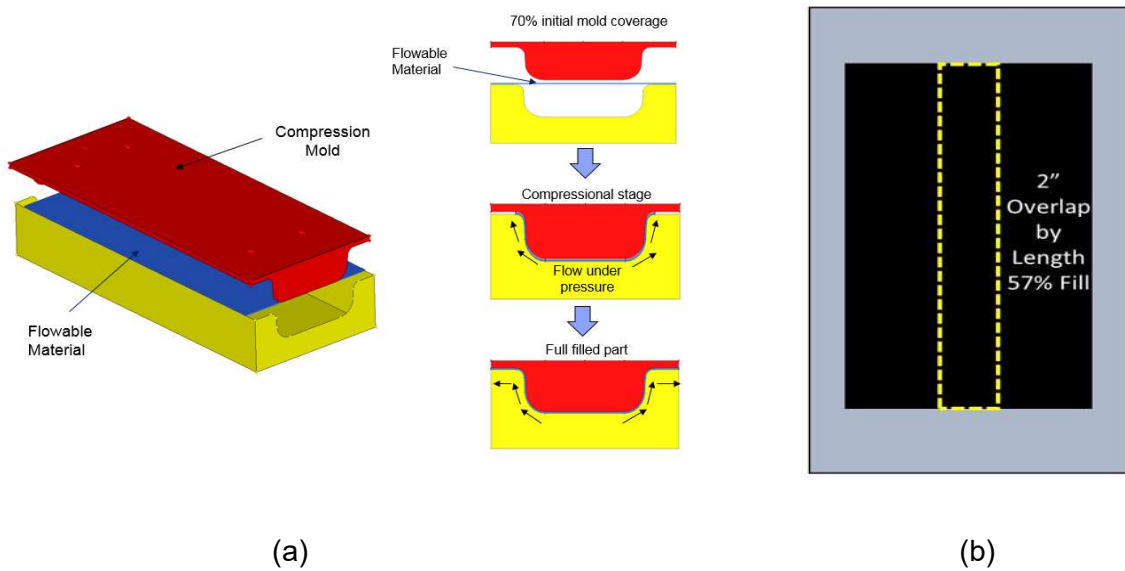
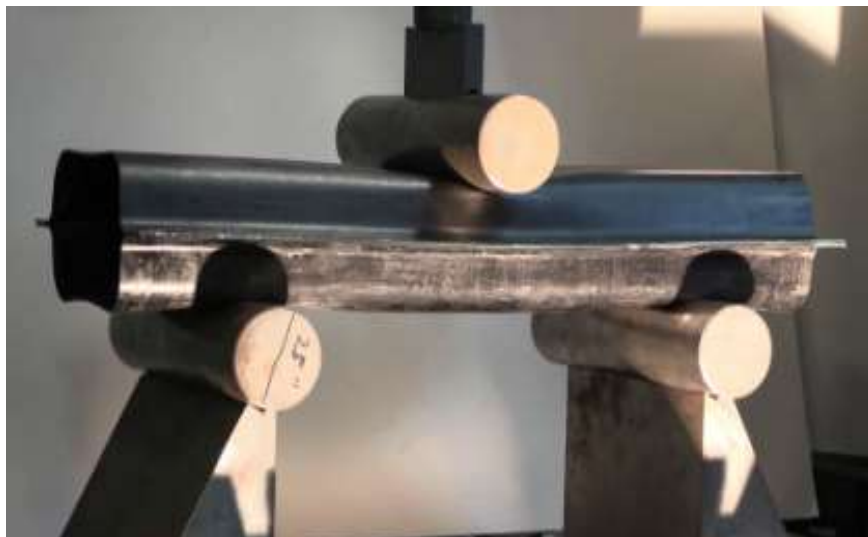
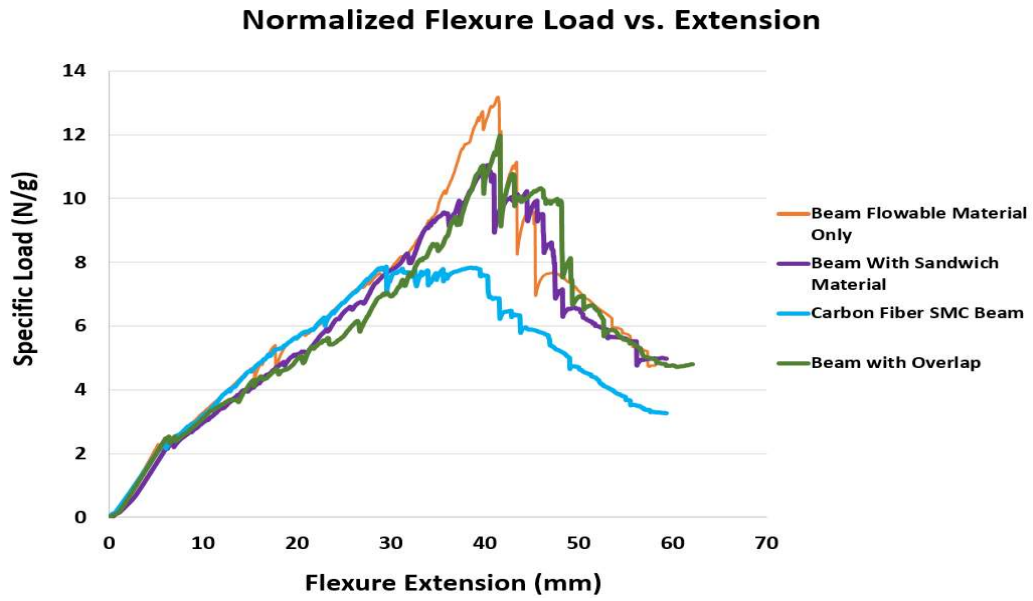


Figure 15. (a) The beam tool of molding flowable material. (b) Overlapped charge



(a)



(b)

Figure 16. (a) Beam three-point bend test setup. (b) Specific load vs. flexure extension curves for all tested beams.

CONCLUSIONS

2. A series of tests was conducted to establish the range of fiber length distributions that can enable flowability while maintaining the reinforcing functions of the fibers in an epoxy polymeric matrix
3. A perforating machine was designed and built to produce carbon fiber preregs with a predetermined fiber length distribution. The machine included a cutting head with 76 toothed blades. The blades' teeth were 1 mm wide and 9.5 mm apart. The design of the cutting head was such that 90 wt% of the fibers were 85 mm long and 10 wt% were 10 mm long.
4. Various carbon fiber preregs were studied for flowability and cure time. The down-selected carbon fiber prepreg was able to deliver molding with a charge pattern of 70% surface coverage and a cure time of less than 3 min.
5. Using the selected carbon fiber prepreg, 12X12 inch plaques were molded for testing at the coupon level as well as the plaque level. The test results showed that the perforated material has a 25% reduction in tensile strength at break compared to as received prepreg. However, the tests also showed that the tensile modulus remains almost at the same level as the as received prepreg. This observation is important because the design of many vehicle panels is modulus driven.
6. Using an epoxy polymer matrix in combination with hollow glass microspheres, a lightweight flowable core was formulated and produced. The core material was prepared such that it would have the same rheological behavior as the carbon fiber prepreg with the cut fibers.
7. The core material was used in combination with the perforated carbon fiber prepreg to produce a sandwich structure. The thickness ratios were designed to deliver various mechanical and physical properties.
8. With a thermal expansion less than steel and a molding shrinkage of less than 0.23%, this family of materials can deliver dimensionally stable parts. It was also demonstrated that these materials can be molded at 400 psi without loss of properties, which enables the use of low cost tooling.
9. Composite beams were also produced using these materials and demonstrated that net shape molding with no offal is another advantage of this methodology. The next step for this project is to identify a component application to validate these findings.

ACKNOWLEDGMENTS

The authors would like to acknowledge Nicole Ellison of General Motors for her sample preparation work at early stages of this project.

REFERENCES

1. Warren, C. D.; Paulauskas, F. L.; Baker, F. S.; Eberle, C. C.; Naskar, A. Development of Commodity Grade, Lower Cost Carbon Fiber-Commercial Applications, SAMPE J. 2009, 45, 24.
2. Baker, F. S.; Baker, D. A.; Gallego, N. C. Advancement in the Manufacturing of Textile Grade PAN-Precursors for Low-Cost Carbon Fiber: Morphological Evaluations, Proceeding, SAMPE '10 Conference and Exhibition, Seattle, WA, May, 17–20, 2010.
3. Vautard, F; Naskar, A.; Paulauski, F.L.; Ozcan, S., Surface Treatment of Carbon Fibers by Continuous Gaseous System, Proceedings, SAMPE 2011, Conference and Exhibition, Long Beach, CA, 23-26 May 2011.
4. Baker, D. A.; Gallego, N. C.; Baker, F. S., On the Characterization and Spinning of an Organic-Purified Lignin Towards the Manufacture of Low-Cost Carbon Fiber," J. Appl. Polymer Sci, 2011, DOI: 10.1002/app.33596

5. Baker, D. A.; Rials, T. G., Recent Advances in Low-Cost Carbon Fiber Manufacture From Lignin, *Applied Polymer Science*, 2013, DOI: 10.1002/APP.39273.
6. Lee, H.; Hugh, M.; Yoon, J.; Lee, D; Kim, S.; Kang, S., Fabrication of Carbon Fiber SMC Composites with Vinyl Ester and Effect of Carbon Fiber on Mechanical Properties, *Carbon Letters*, Vol.22,101-104 (2017)
7. Eksi, S.; Genel, K., Comparison of Mechanical Properties of Unidirectional and Woven Carbon, Glass and Aramid Fiber Reinforced Epoxy Composites, Special issue of the 3rd International Conference on Computational and Experimental Science and Engineering (ICCESEN 2016), DOI: 10.12693/APhysPolA.132.879
8. Mrse, M; Piggott, M.R, Compressive Properties of Unidirectional Carbon Fiber Laminates: II. The Effects of Unintentional and Intentional Fiber Misalignments, *Composites Science and Technology*, Volume 46, Issue 3, 1993, Pages 219-227
9. Arteiro, A.; Catalanotti, G.; Melro, A.R., Linde, P.; Camanho, P.P., Micro-Mechanical Analysis of the Effect of Ply Thickness on the Transverse Compressive Strength of Polymer Composites, *Composites Part A: Applied Science and Manufacturing*, Volume 79, December 2015, Pages 127-137
10. Wulfsberga, J.; Herrmannb, A.; Ziegmannc,G.; Lonsdorferb, G.; Stößd, N. Fettea, M., Combination of Carbon Fiber Sheet Molding Compound and Prepreg Compression Molding In Aerospace Industry, 11th International Conference on Technology of Plasticity, Nagoya Congress Center, Nagoya, Japan ICTP 2014, 19-24 October 2014,
11. Miwa, M.; Endo, I., Critical Fiber Length and Tensile Strength for Carbon Fiber-Epoxy Composites, *Journal of Materials Science*, March 1994, Volume 29, Issue 5, pp 1174–1178.
12. Santulli, C, Critical Length Measurements in Carbon Fibers During Single Fiber Fragmentation Tests Using Acoustic Emission, *Journal of Materials Science*, April 2004, 39(8):2905- 2907,
13. Lacroix,T.; Tilmans,B.; Keunings, R.; Desaegeer, M.; Verpoest, I., Modelling of Critical Fiber Length and Interfacial De-Bonding in the Fragmentation Testing of Polymer Composites, *Composites Science and Technology*, Volume 43, Issue 4, 1992, Pages 379-387.
14. Kia, H. G., Modification of Continuous Carbon Fibers During Precursor Formation For Composites Having Enhanced Moldability, US Patent 9896783, Issue Date: 2/20/2018.
15. Kia, H. G., Modification of Continuous Carbon Fibers During Manufacturing for Composites Having Enhanced Moldability, US Patent 10113250, Issue Date: 10/30/2018.
16. Kia, H. G.; Zhao, S. X., Modification of Continuous Carbon Fibers During Precursor Formation for Composites Having Enhanced Moldability, Filing date: 8/24/2017

17. Kia, H.G.; Ellison, N.D.; Zhao, S.X.; Carbon Fiber Pre-Pregs and Methods For Manufacturing Thereof, US Patent Application 20180016740, Publication Date, January 2018
18. Dillon, G.P.; Barsoum, M., Characterization of Stretch Broken Carbon Fiber Materials for Automated Forming, SAMPE 2005, May 1-5, Long Beach CA,
19. Jacobsen, G.; Schimpf, W.C., Process Development and Characterization of Stretch Broken Carbon Fiber Materials – SAMPE2009 Spring Symposium, Volume 54, May 18-21, 2009 Baltimore, MD
20. Kia, H. G.; Zhao, S. X., Equipment for Perforated Pre-impregnated Reinforcement Materials, Filing date: 12/8/2017

Appendix

staggered cut pattern on uni-directional prepreg

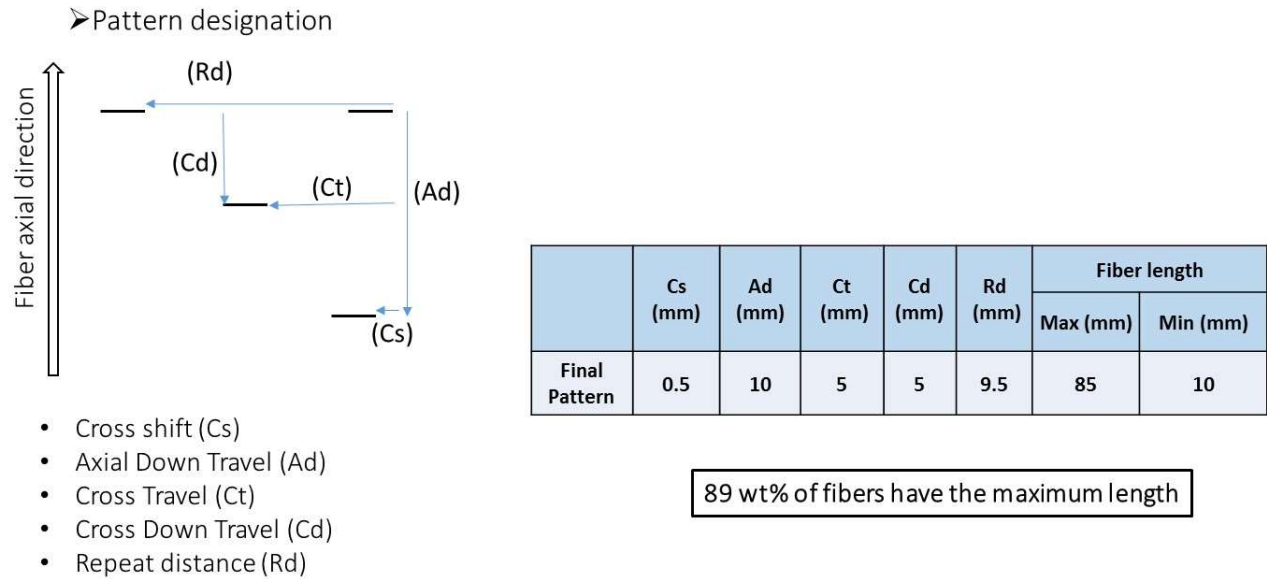


Figure A1. The staggered cut pattern on unidirectional prepreg

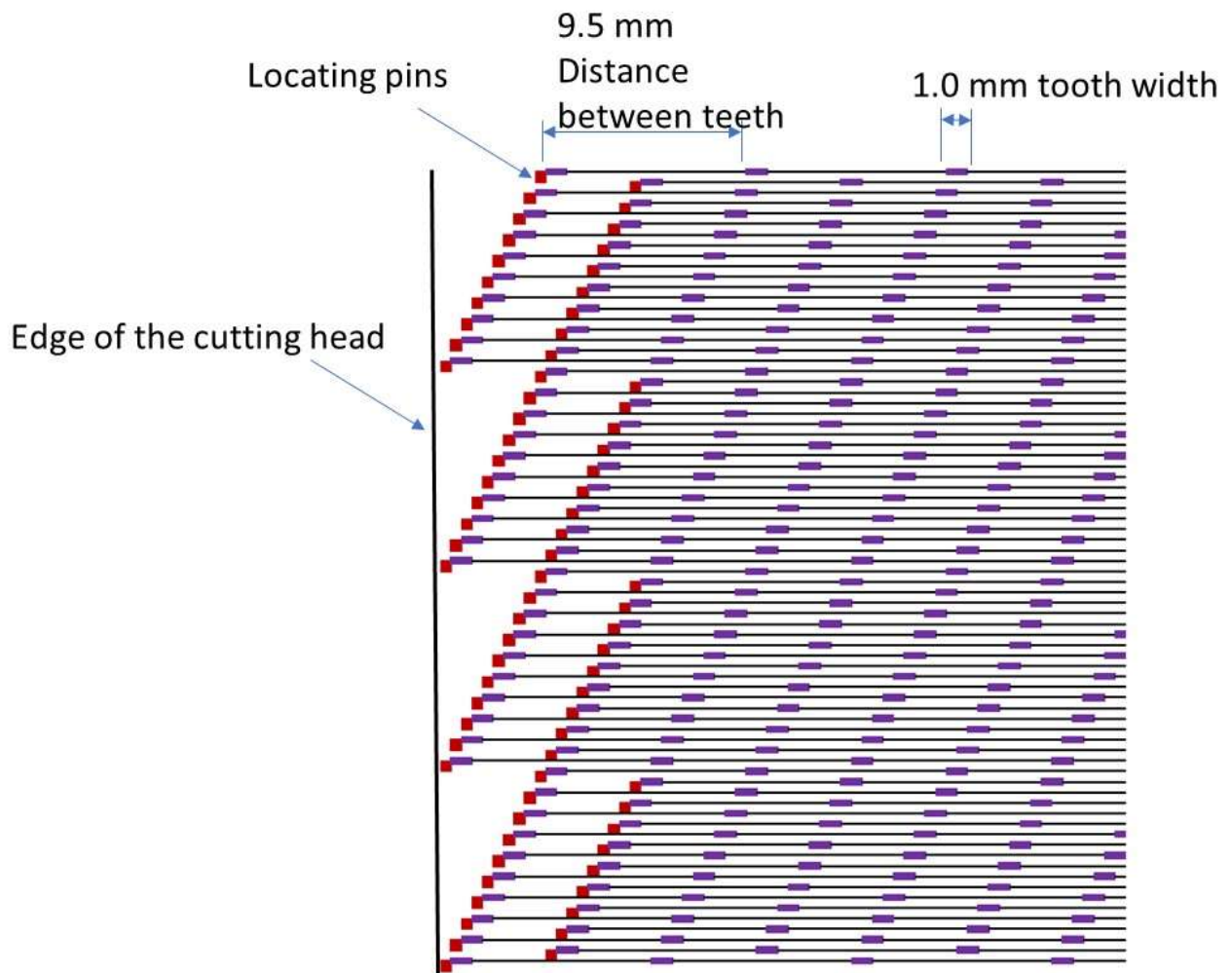


Figure A2. The schematic representation of the cutting head blades

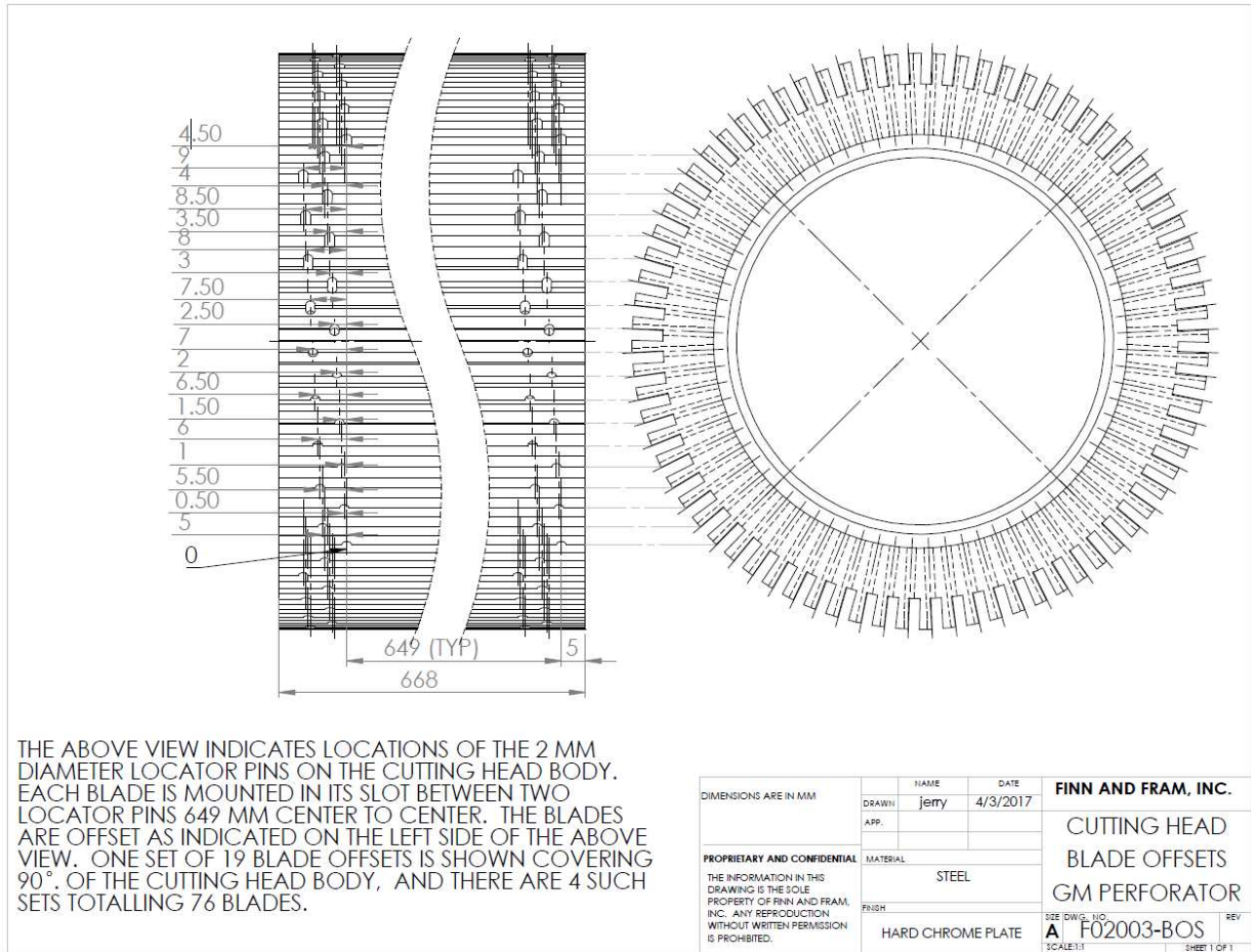


Figure A3. The schematic representation of the cutting head blade offset pattern

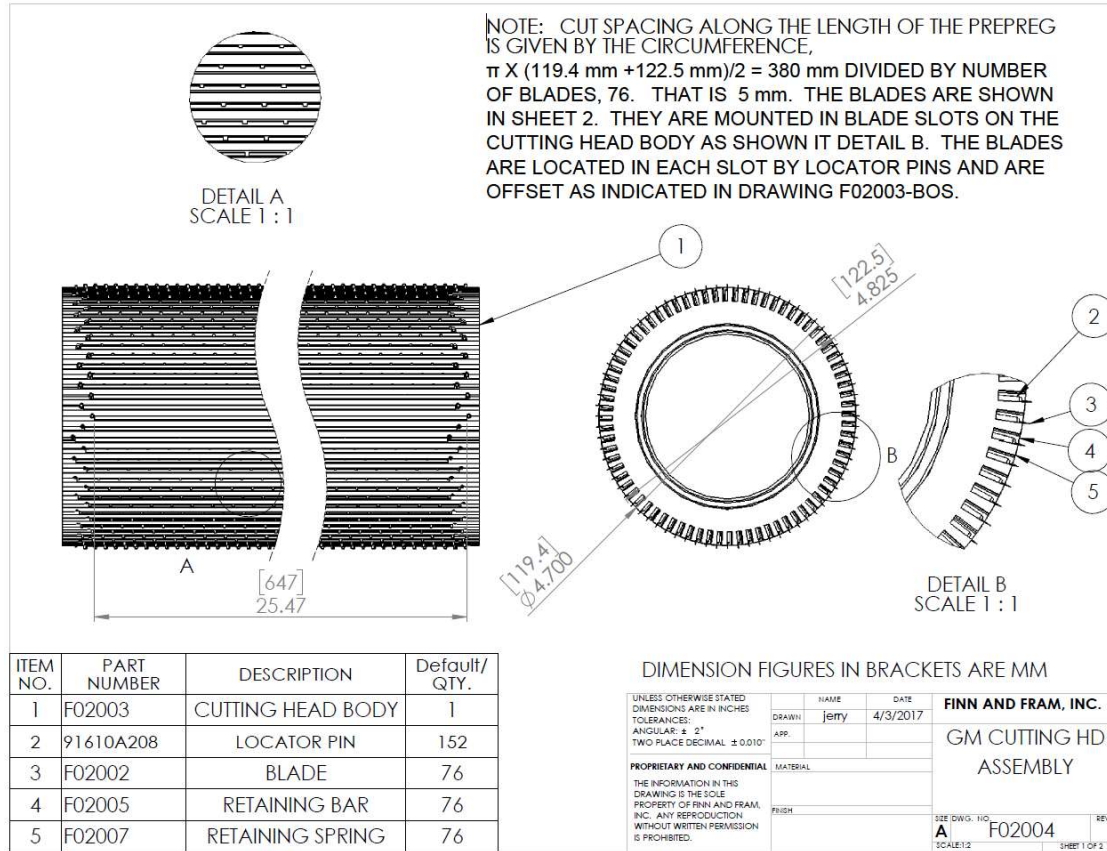


Figure A4. The schematic representation of the cutting head assembly

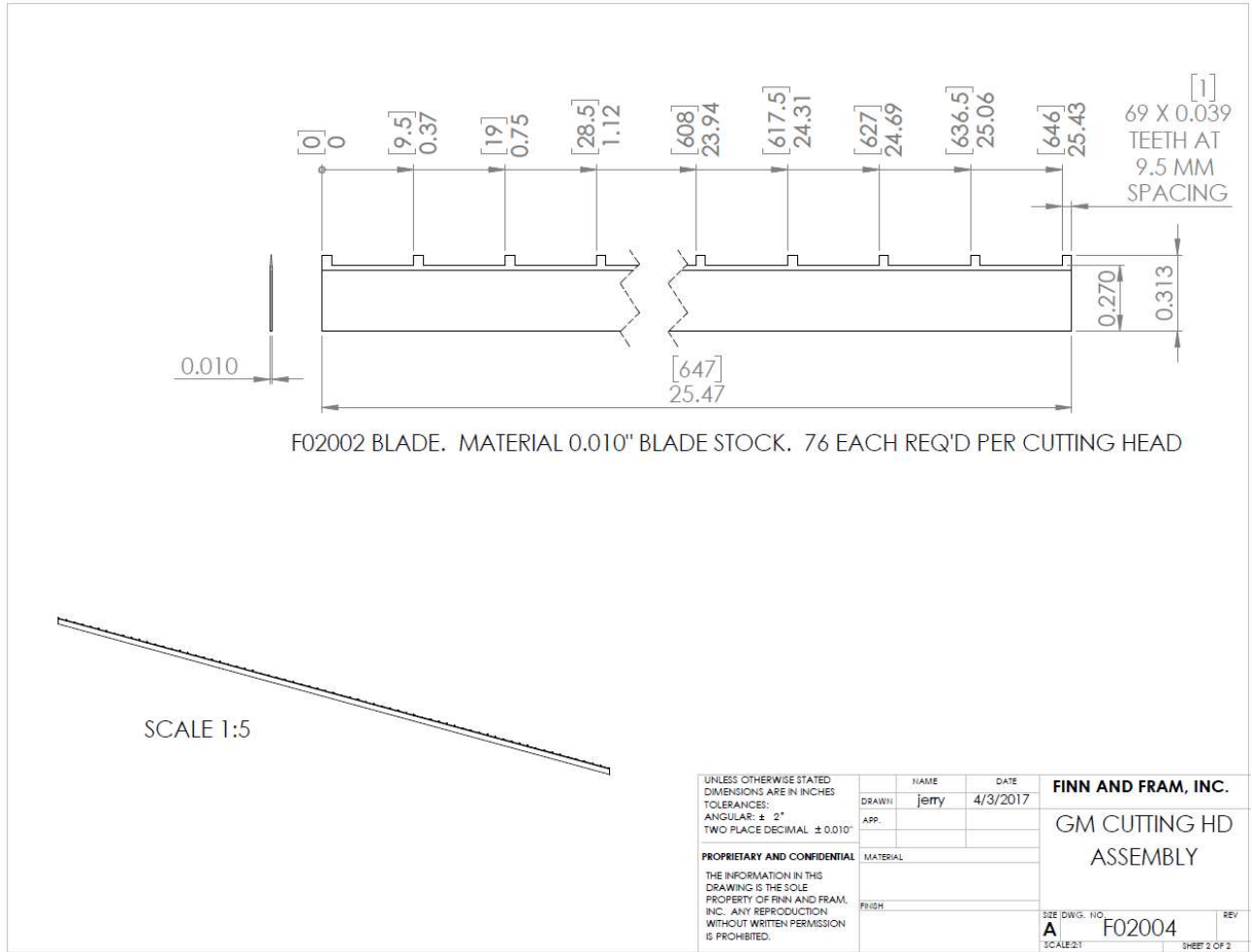


Figure A5. The schematic representation of the cutting head blade teeth location

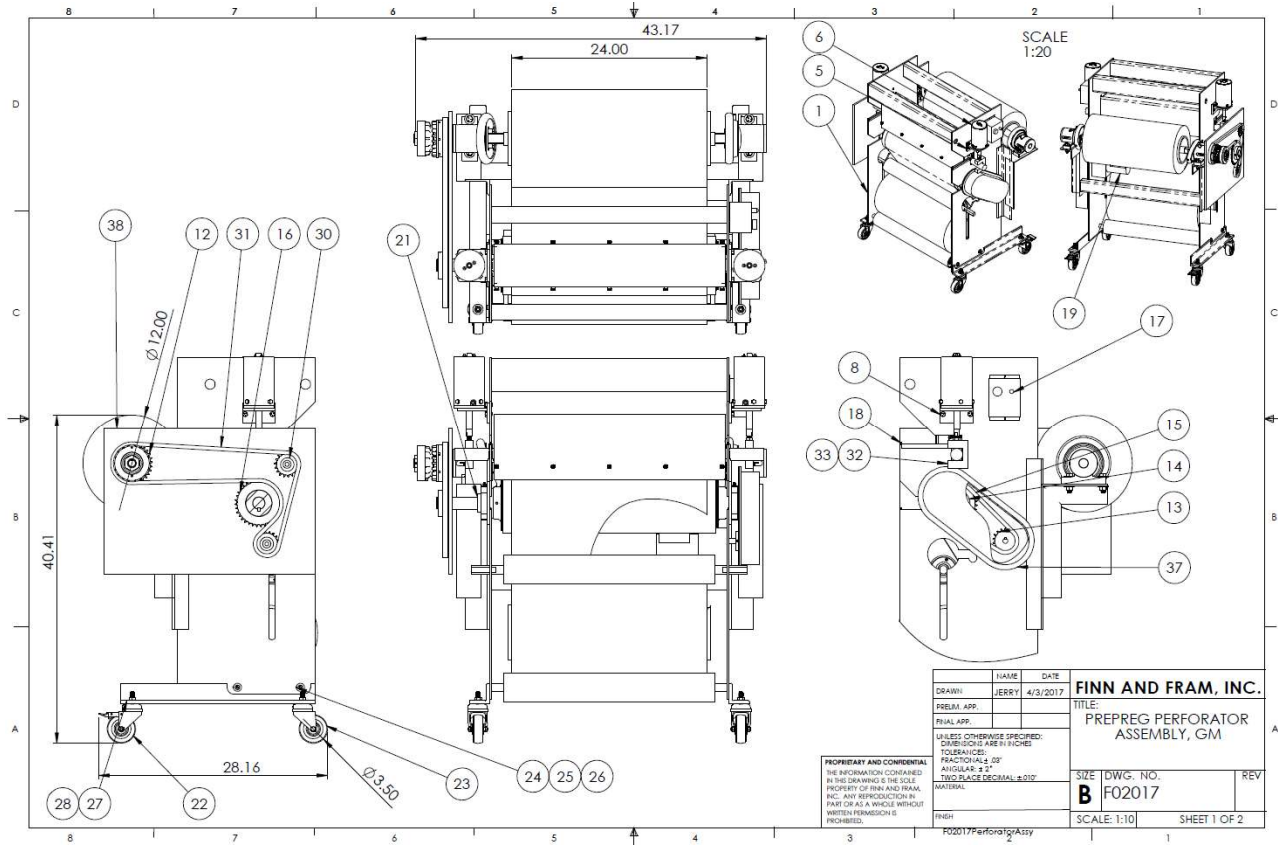


Figure A6a. The schematic representation of the perforating machine as designed (part 1)

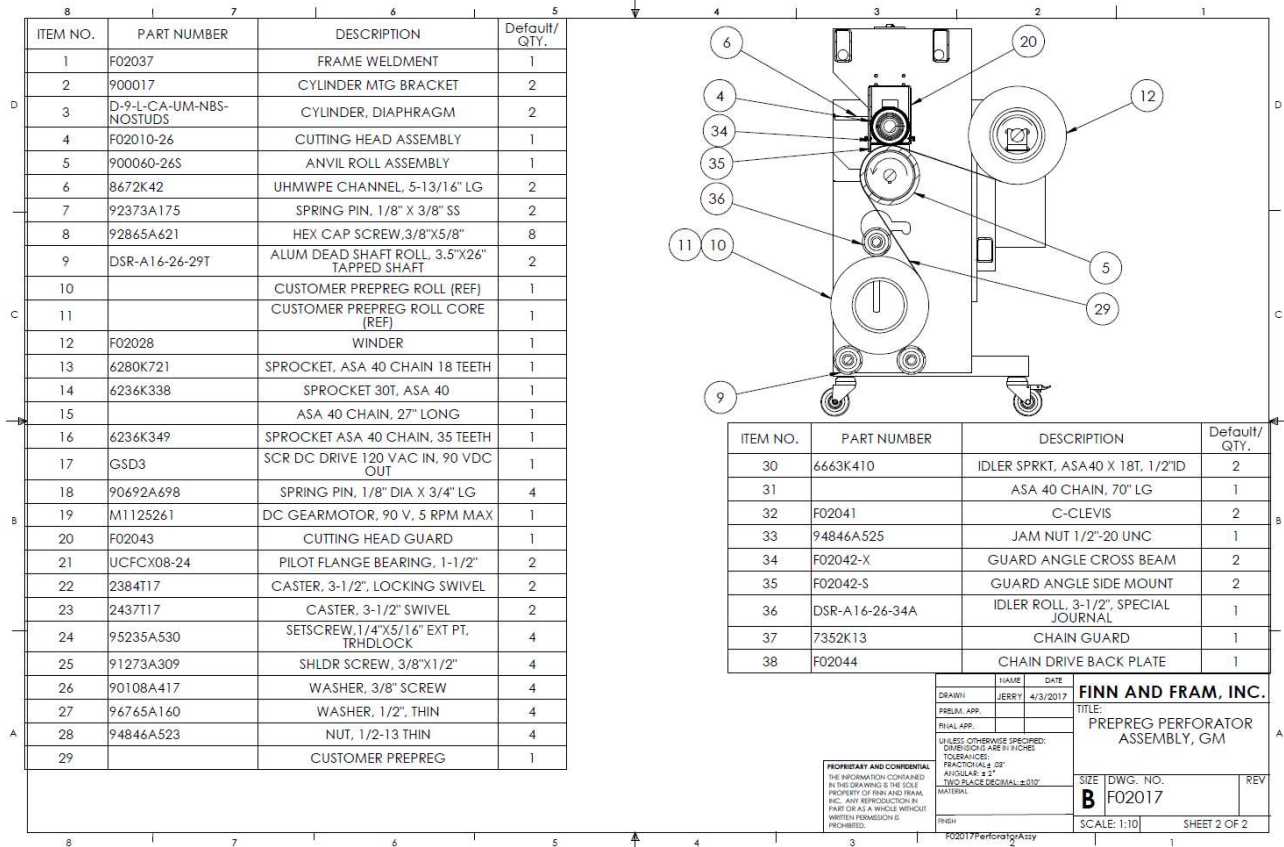


Figure A6b. The schematic representation of the perforating machine as designed (part 2)

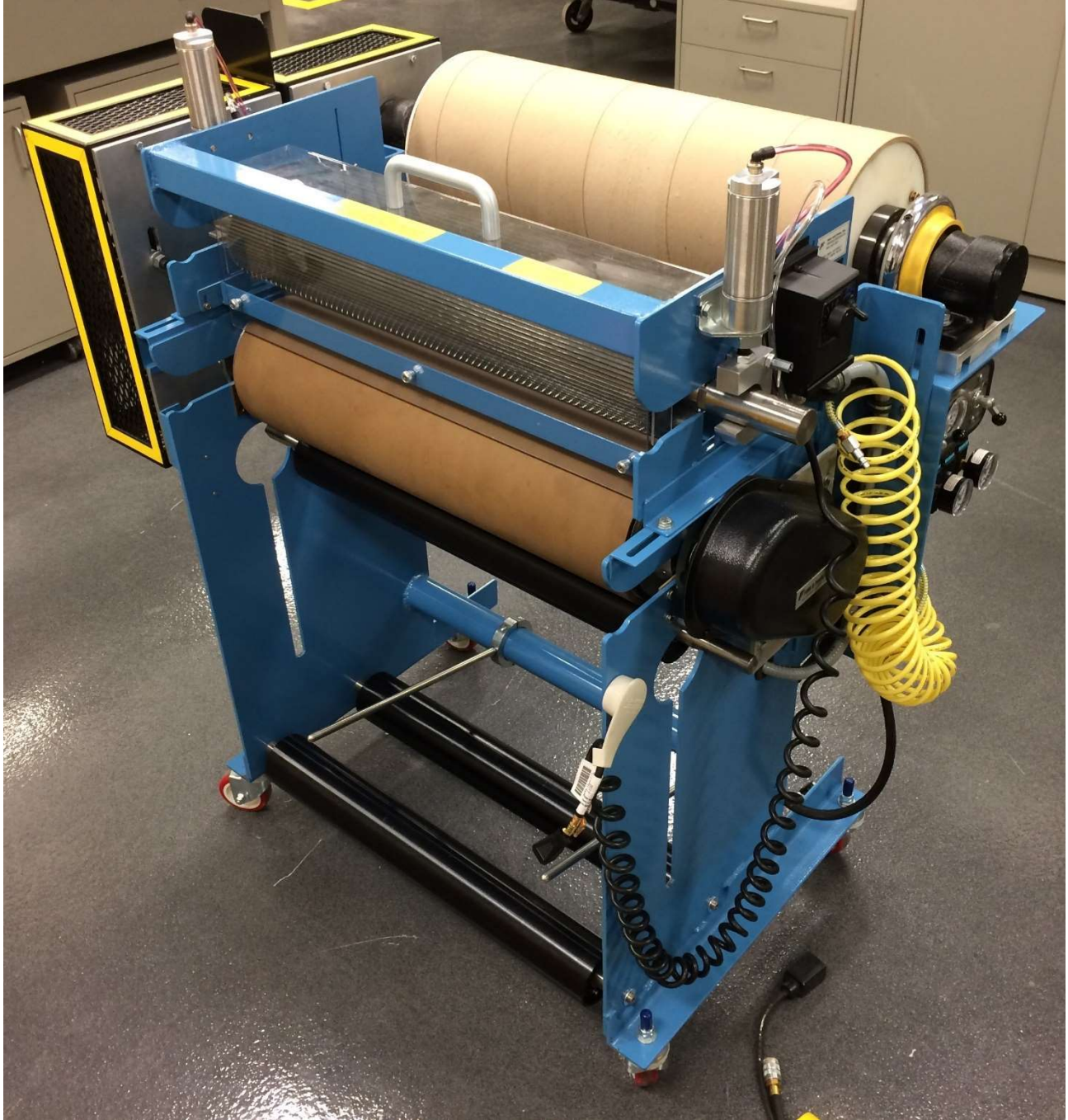


Figure A7. The final perforating machine as built per specification.

